Appl. Phys. B 89, 299–304 (2007)
DOI: 10.1007/s00340-007-2794-4

Applied Physics B
Lasers and Optics

N.P. BARNES[1,✉]
B.M. WALSH[1]
D.J. REICHLE[1]
R.J. DEYOUNG[1]
SHIBIN JIANG[2]

Tm:germanate fiber laser: tuning and Q-switching

[1] NASA Langley Research Center, Hampton, VA 23681, USA
[2] NP Photonics, Tucson, AZ, USA

Received: 12 June 2007/Revised version: 6 August 2007
Published online: 21 October 2007 •

ABSTRACT A Tm:germanate fiber laser produced > 0.25 mJ/pulse in a 45 ns pulse. It is capable of producing multiple Q-switched pulses from a single pump pulse. With the addition of a diffraction grating, Tm:germanate fiber lasers produced a wide, but length dependent, tuning range. By selecting the fiber length, the tuning range extends from 1.88 to 2.04 μm. These traits make Tm:germanate lasers suitable for remote sensing of water vapor.

PACS 42.55.Wd; 42.55.Xi

1 Introduction

Remote sensing of water vapor can be accomplished employing a DIAL technique. This requires a laser that is tunable around a strong water vapor absorption feature. The DIAL instrument transmits a pair of laser pulses. The first pulse is tuned to the peak of the absorption feature. The second laser pulse is tuned to a wavelength well away from the water vapor absorption feature. Aerosol particles in the atmosphere scatter some of the transmitted laser pulse back to the DIAL receiver. Water vapor concentration can be determined as a function of range by taking the logarithm of the ratio of the back scattered returns. Measurements under arid atmospheric conditions or measurements over short ranges benefit by probing very strong water vapor absorption features. Strong absorption features can be found in the vicinity of 1.8 μm. Because these absorption features are narrow, the laser spectral bandwidth must be much narrower than the water vapor absorption features. For best results, the pair of laser pulses should be in close temporal proximity in order to probe the same segment of the atmosphere. For short ranges, only a modest amount of laser energy is required. However, for good range resolved measurements, the Q-switched pulse length should be short, less than 100 ns.

Water vapor is the most radiatively active gas in the atmosphere, both capturing and transporting energy within the atmosphere. In turn, this influences weather patterns and ultimately climate. The concentration of water vapor is highly variable in both time and space, therefore making measurements of concentration difficult. Nevertheless, to predict future weather with meaningful accuracy, a multitude of real-time measurements need to be taken. These data serve as input for atmospheric models to accurately predict weather. Even short range weather predictions can have major economic consequences.

A weather station, including a water vapor lidar, could continuously determine the water vapor concentration through out the atmosphere about the station. Lidar can not only give the water vapor concentration but also measure aerosol profiles and cloud heights. These data are valuable model inputs. Such a lidar would employ the differential absorption lidar, DIAL, technique, described above. There is a plethora of water vapor absorption lines that could be employed. However, it is prudent to employ wavelengths in the eye-safe region of the spectrum to avoid interference with aircraft.

This same technology could be employed on Mars to determine atmospheric water vapor profiles. Although the concentration of water vapor is very low, there is still sufficient vapor to form hazes, ground fog and frost. An exchange of water vapor exists between the Northern pole and the atmosphere, which grows and recedes with the seasons. However, the arid conditions strongly favor the use of strong absorption features. Long-term interest exists in the question of whether life exists on Mars today in any form. Life as known on Planet Earth requires water. Thus, there is great interest in determining the concentration and extent of present day water on the surface. The DIAL technique could be utilized to measure the processes that determine the distribution of water vapor. Perhaps this would indicate where sources and sinks of water vapor exist. In turn, this could be sites where life on Mars might be found.

Both the Earth and Mars applications require a laser system that is rugged, dependable, low mass, efficient and with a long service lifetime. Fiber lasers have matured to the point that they can be considered for these applications. A narrow line, tunable, efficient, fiber laser could fulfill the challenging conditions demanded by these applications. Such a laser would need a linewidth on the order of a picometer. Also it should be rapidly tunable to the peak of a strong water vapor absorption line and then several tens picometers away to some wavelength region where no water vapor absorption occurs. Fiber lasers can also be low-mass, rugged, devices with

✉ Fax: +1 757 864-8828, E-mail: n.p.barnes@larc.nasa.gov

high efficiency. If the Tm:germanate fiber laser achieved the desired performance, the system can be made more rugged by using fiber optic components for tuning, line narrowing, and Q-switching.

A Tm:germanate laser, tunable around 1.9 μm, can fulfill the requirements for a water vapor DIAL system. To demonstrate the applicability of Tm:germanate for remote sensing, this material was fabricated into a double-clad fiber laser and diode pumped. Spectroscopic parameters of the Tm:germanate have been measured [1, 2]. The selection of Tm:germanate was dictated by efficiency and tuning considerations. Other Tm fiber choices include Tm:silica and Tm:ZBLAN. Unfortunately, there are some potential problems with both of these choices.

2 Material choices

To be efficient, a diode-pumped laser should have a quantum efficiency approaching 2.0. An energy level diagram appears in Fig. 1. Laser diodes are commercially available to pump the $^3H_4$ manifold but not the $^3F_4$ manifold. Consequently, diode-pumped Tm lasers commonly pump the $^3H_4$ manifold. If a single pump photon produces a single active atom in the upper laser manifold, the laser efficiency is limited by a ratio of photon energies, λ_P/λ_L. If commercially available laser diodes at ≈ 0.79 μm are employed for pumping, this ratio is ≈ 0.4. Fortunately, self quenching can increase this efficiency significantly. Through the self-quenching process, a Tm atom in the $^3H_4$ manifold can interact with a nearby Tm atom in the $^3H_6$ manifold to transfer both Tm atoms into the $^3F_4$ manifold, the upper laser manifold. This process is in competition with natural decay of the $^3H_4$ manifold. Natural decay of the $^3H_4$ manifold is a result of both radiative and nonradiative transitions. However, nonradiative transitions are usually dominant. When self quenching is competitive, the laser efficiency becomes $\eta_Q\lambda_P/\lambda_L$. The quantum efficiency, η_Q, is the average number of Tm atoms promoted to the $^3F_4$ manifold for each absorbed photon. In an ideal circumstance, the quantum efficiency approaches 2.0.

Nonradiative transitions can be minimized by a judicious choice of laser material. Nonradiative transitions require the emission of phonons so that energy is conserved. The required number of phonons is approximately the energy gap to the next lower manifold divided by the maximum phonon energy.

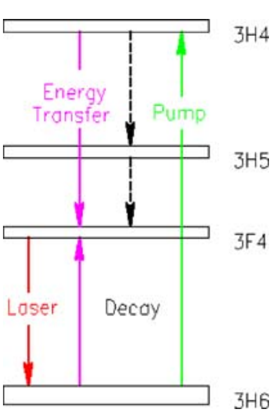

FIGURE 1 Energy manifolds of Tm

As a rule of thumb, if the required number of phonons is ≈ 5 or greater, nonradiative transitions will not be competitive. The energy gap between the $^3H_4$ and $^3H_5$ manifolds is approximately 4500 cm^{-1}. Thus, the maximum phonon energy of the selected laser material should be less than 900 cm^{-1}. Maximum phonon energy of germanate glasses were found to be in the range of 800 to 975 cm^{-1} [3] by looking at high lying levels. Similar results were found for GeO_2–Na_2O glasses and for GeO_2–Cs_2O [4]. For comparison, maximum phonon energy of silica, and ZBLAN are approximately 1100 and 500 cm^{-1}, respectively. From a phonon energy point of view, germanate and ZBLAN laser materials are favored.

Germanate is favored because it is more durable than ZBLAN. Often fiber lasers are relatively long, in excess of a meter. To package these lasers in a reasonable sized package, the fiber is coiled. Coiling puts stress on the fiber, endangering its reliability. For ZBLAN, the smallest recommended coil diameter is about 0.5 m. This is roughly fivefold larger than silica. From the reliability point of view, silica and germanate are favored. In addition, germanate glasses tend to have better infrared transmission than silica glasses [3].

A few Tm:fiber lasers with different germanate glass compositions have been demonstrated. The emission spectra of GeO_2–PbO–Nb_2O_5 was measured and used in a Judd–Ofelt analysis to determine lifetime and emission cross section [5]. A 1.9 μm Tm:germanate fiber laser was demonstrated [6].

3 Experimental arrangement

A double end pumping arrangement yielded a nearly uniform inversion profile. The laser diodes were nominally at 0.792 μm. The output beam profile was an 11.0 by 11.0 mm square pattern. The pump beam on both ends passed through a dichroic mirror that transmitted pump wavelengths but reflected laser wavelengths. A 20 mm focal length lens focused the pump radiation onto the 143 μm diameter, 0.216 numerical aperture, inner cladding of the Tm:germanate fiber. The Tm:germanate fiber has a 35 μm core and a 0.044 numerical aperture. An advantage of the Tm:germanate is its ability to tolerate high Tm concentrations. Because of this tolerance, a Tm concentration of 0.04 was used. Experiments [7] indicated that Tm concentrations of 0.04 or more promoted self quenching strongly, concomitantly improving laser efficiency.

A TeO_2 acousto-optic modulator served to Q-switch the laser. TeO_2 has several advantages, including relatively large photo elastic constants. This is especially important in this case because the diffraction efficiency scales approximately as λ^{-2} where λ is the wavelength. Therefore, the large photo elastic constants compensate for the longer wavelengths. In addition, the effective diffraction efficiency of the TeO_2 modulator is only weakly dependent on the polarization. This is important for unpolarized fiber lasers. The TeO_2 modulator operated at a radio frequency power at 24 MHz, favoring Raman Nath operation.

Tuning was accomplished using a 600 g/mm grating. The grating was gold coated and blazed for operation around 1.8 μm. To incorporate the grating into the laser resonator, the highly reflective end mirror was replaced by a 160 mm focal length lens. This lens produced a beam waist on the grating

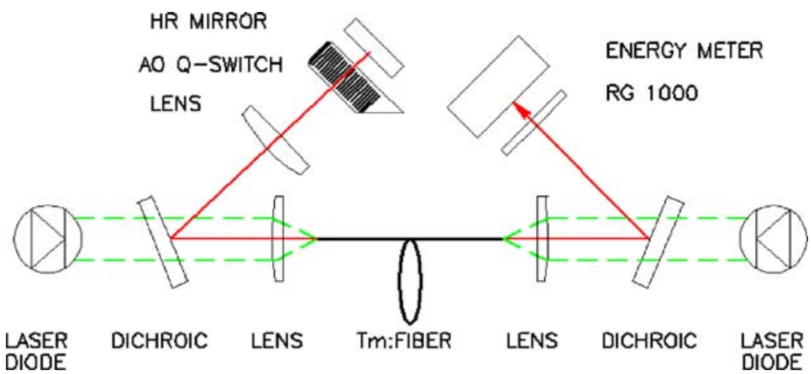

FIGURE 2 Double-end pumping of Tm:germanate fiber laser

which nearly filled the width of the diffraction grating. The output coupler is the Fresnel reflection from the end of the cleaved Tm:germanate fiber laser. With the relatively high index of refraction of the germanate glass, the output reflectivity is approximately 0.06. To obtain a narrower spectral output, a coated, 2.0 mm etalon was placed near the grating.

4 Experimental results

Normal mode operation achieved a slope efficiency of 0.285, diode output power to laser output energy. In anticipation of Q-switching, two lenses were incorporated in the resonator. A 20 mm focal length lens essentially collimated the laser beam as it emerged from the fiber. A 100 mm focal length lens produced a waist close to the acousto optic modulator, providing a short opening time interval. The Tm:germanate fiber laser generated 0.293 mJ/pulse when operated normal mode with a 5.0 ms current pulse length. The laser performance is displayed in Fig. 3. The threshold is 53.5 mJ and the slope efficiency is 0.285. The limiting efficiency factor is coupling the pump light into the inner cladding. For this fiber, the inner cladding diameter is 143 μm and its numerical aperture is 0.216. Although the inner cladding is larger than previous Tm:germanate fibers, the launch efficiency is calculated to be only 0.4.

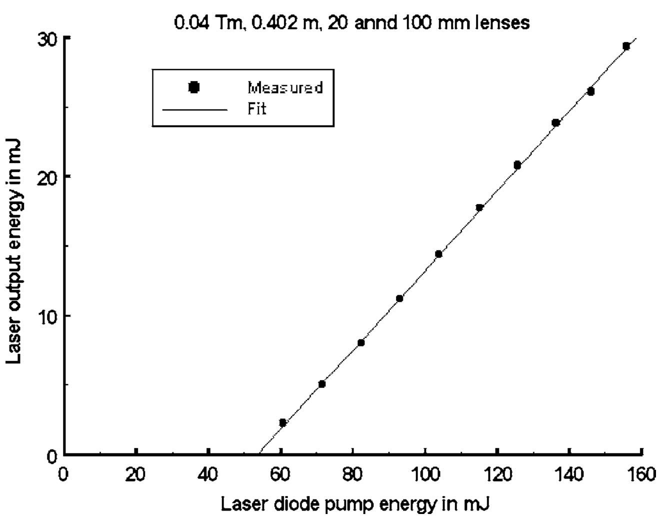

FIGURE 3 Normal mode operation of the Tm:germanate fiber laser demonstrating slope efficiency of 0.285, laser output energy to diode pump efficiency

When Q-switched, Tm:germanate could produce in excess of 0.25 mJ in a 50 ns pulse length. Normal mode and Q-switched performance appear in Figs. 4 and 5 for the same current range and several pump pulse lengths. The Q-switched pulse energy was restricted to ≈ 0.25 mJ in a single pulse to avoid laser induced damage. As expected, thresholds for nor-

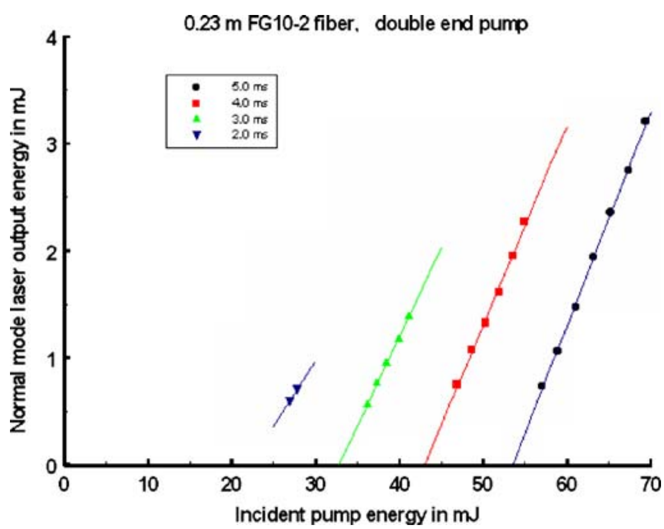

FIGURE 4 Normal mode laser output energy vs. diode output energy for 2.0, 3.0, 4.0, and 5.0 ms pump pulse lengths

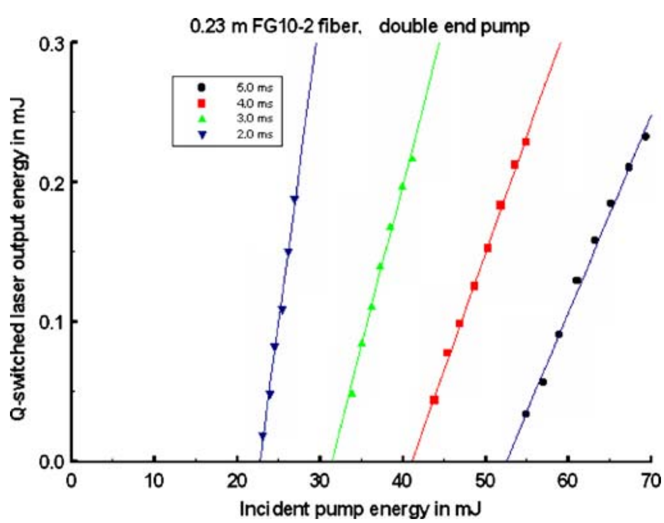

FIGURE 5 Q-switched laser output energy vs. diode pump energy for 2.0, 3.0, 4.0, and 5.0 ms pump pulse lengths

mal mode and Q-switched operation are nearly equal and increase as the pump pulse length increases. Slope efficiency for normal mode operation increases with increasing pump pulse length. This behavior is primarily a result of laser operation occurring over an increasing fraction of the pump pulse. Conversely, slope efficiency for Q-switched operation decreases with increasing pump pulse length. This is a result of decreasing storage efficiency.

The slope efficiency for Q-switched operation is directly proportional to the storage efficiency. The storage efficiency is the fraction of the active atoms promoted to the upper laser manifold that remain in the upper laser manifold at the time of the Q-switch opening. The storage efficiency can be calculated under an assumption of linear loss only or under an assumption of nonlinear loss. Linear loss can result from both radiative and nonradiative decay. Conversely, nonlinear loss can result from up conversion or from amplified spontaneous emission. The storage efficiency, η_S, can be calculated both for linear and nonlinear approximations. Solutions are, respectively [8]

$$\eta_S = (\tau_2/\tau_I)(1-\exp(-\tau_I/\tau_2)) , \quad \text{linear}$$

$$\eta_S = 2(\tau/\tau_I)\frac{1-\exp(-D\tau_I/\tau)}{(1+D)-(1-D)\exp(-D\tau_I/\tau)} ,$$

$$1/\tau = 1/\tau_2 - R/N_S C_T ,$$

$$D = (1+4\beta R\tau^2)^{1/2} , \quad \text{nonlinear} .$$

In these expressions, τ_2 and τ_I are the upper laser manifold lifetime and pump pulse length, respectively. R is the pumping rate, the number density of atoms delivered to the upper laser manifold per second. C_T is the concentration of Tm and N_S is the number density of possible Tm sites. Thus, $C_T N_S$ is the number density of Tm atoms. β is the nonlinear loss term that results from up conversion or amplified spontaneous emission. For up conversion, β is given by $(2-\eta_Q)P_{22}C_T N_S$. Here η_Q is the quantum efficiency and P_{22} is the up conversion parameter.

A nonlinear loss causes a decrease in the effective storage lifetime and a nonlinear dependence of the population density on the pump energy. Fluorescence originating from the $^3F_4$ manifold was monitored by observing radiation escaping through the side of the fiber. Fluorescence data were gathered for seven different pump levels. Using this data, one can determine the effective lifetime and the population density in the upper laser manifold as a function of the pump energy. Results of these measurements [8] are shown in Fig. 6. The model predicts that the inverse of the lifetime increases linearly as the pump energy increases. Because of this and up conversion losses, the population density of the $^3F_4$ manifold increases more slowly than linearly as the pump energy increases. Both of these predictions are supported by experimental data, shown in Fig. 6.

The existence of a nonlinear loss is also supported by a comparison of the storage efficiency with the Q-switched slope efficiency. In this case, all of the Tm atoms promoted to the upper laser manifold must wait until the Q-switch opens in order to contribute to the laser pulse. Thus, the slope efficiency must be directly proportional to the storage efficiency. Given the parameters obtained from the fluorescence data, one can calculate the storage efficiency parametrically for different pulse lengths. Storage efficiencies under the linear and nonlinear approximations were both calculated. The corresponding measured slope efficiency was then plotted for both sets of calculated storage efficiencies and shown in Fig. 7. When the plotted data are curve fit, the nonlinear loss data fit a straight line that nearly proceeds through the origin. This is the expected behavior. Conversely, the linear loss data can be approximated by a straight line but the line does not visit the neighborhood of the origin. This further supports the nonlinear analysis.

Tm:germanate fiber lasers can be repetitively Q-switched to produce several Q-switched pulses for a single pump pulse. A pair of temporally separated pulses is preferred for some remote sensing applications. Radiative lifetime of the $^3F_4$ manifold, determined by using a Judd and Ofelt analysis, is 4.05 ms, [2]. Measurements of Tm:germanate $^3F_4$ manifold lifetime in samples with low Tm concentration, 0.02 by weight or less, support this determination [2]. However, in a sample with a Tm concentration of 0.04 by

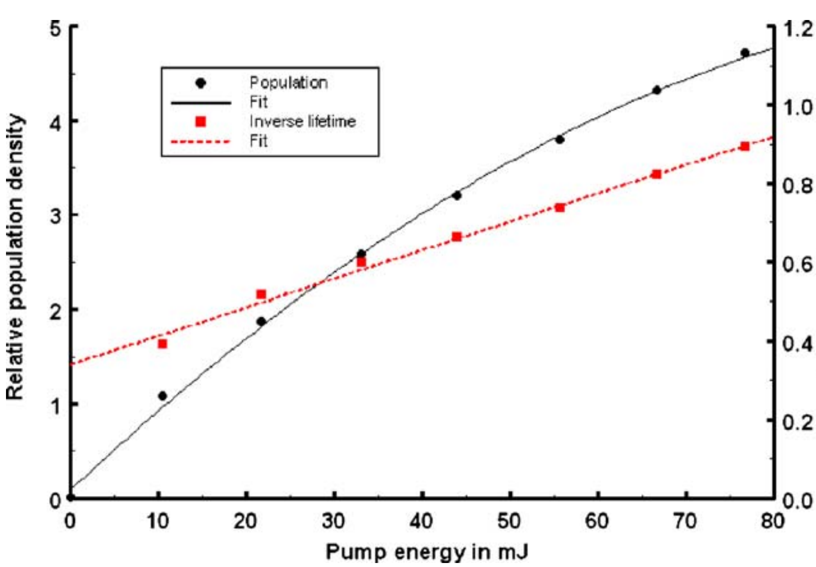

FIGURE 6 Inverse lifetime and relative population density vs. pump energy

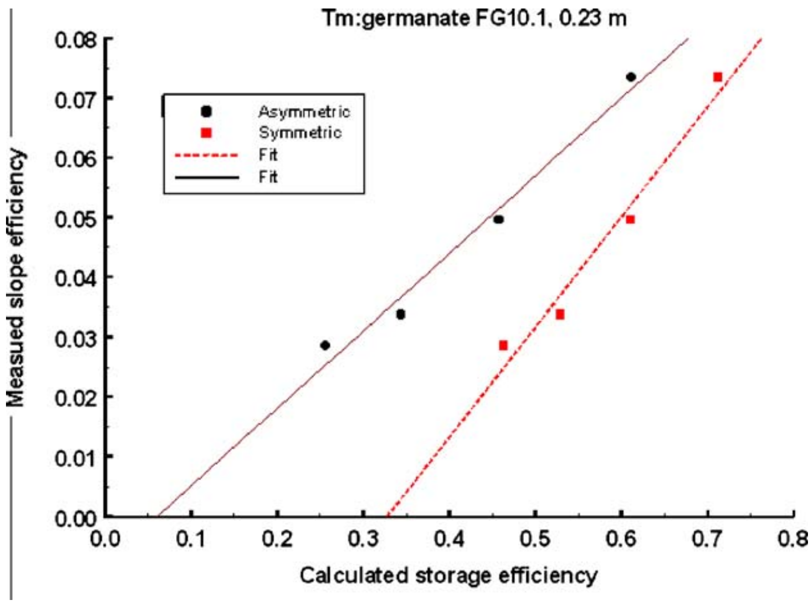

FIGURE 7 Measured slope efficiency vs. calculated storage efficiency for linear and nonlinear loss

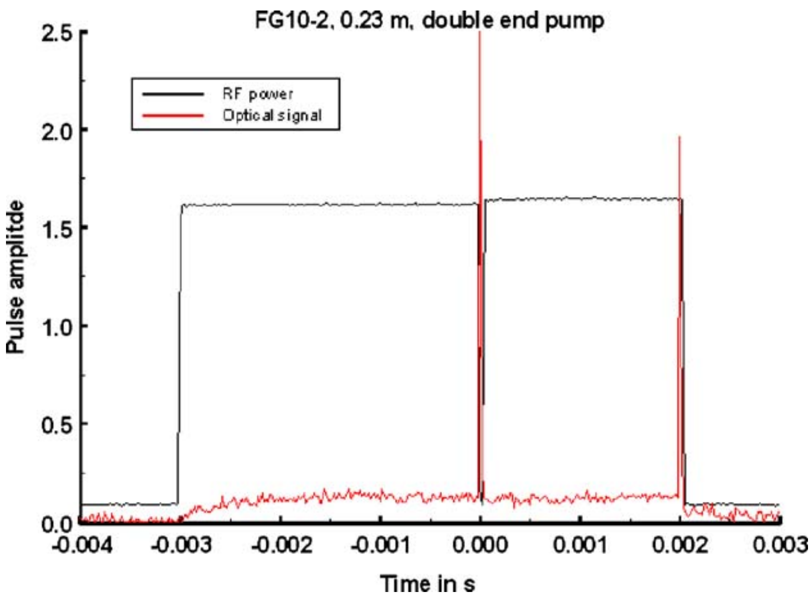

FIGURE 8 Multiple Q-switched pulses during a 5.0 ms pulse

weight, the measured $^3F_4$ manifold lifetime was reduced to be 2.11 ms. The observed behavior of the $^3F_4$ fluorescence lifetime is consistent with the nonlinear loss mechanisms up conversion or amplified spontaneous emission [8]. A lifetime shorter than the expected lifetime suggests that more efficient Q-switched operation is possible using a shorter pump pulses.

A pair of Q-switched pulses can be generated with a single pump pulse. A pair of pulses that are closely spaced in time are favored for lidar DIAL applications so that a similar volume of atmosphere can be sampled. To obtain a pair of pulses, the radio frequency power driving the acousto optic modulator is modulated to be on for 3.0 ms, off for 10 μs, and on again for 2.0 ms. The first Q-switched pulse occurs during the 10 μs gap in the radio frequency power, as shown in Fig. 8. The first pulse contains approximately 0.55 of the total laser output energy. The second Q-switched pulse occurs nominally at the end of the pump pulse and contains approximately 0.45 of the total energy. The amount of energy in each pulse can be adjusted by adjusting the timing of the first pulse.

When the first pulse occurs later in the pump pulse, the energy in the first pulse increases. Conversely, the energy in the second pulse decreases. However, the rate of change of the pulse energy with the temporal location of the first Q-switching time interval is relatively slow. This can be attributed to the length of the pump pulse being long compared with the effective upper laser level lifetime. Although the fraction of the laser output energy contained in the first pulse does not follow a strict linear relation, the rate of change is roughly 83 s^{-1}.

Tm:germanate can be tuned over the range from 1.88 to 2.04 μm. The tuning range of a particular fiber is dependent on the length of the fiber, as shown in Fig. 9. Longer fibers tend to lase at longer wavelengths and vice versa. The laser output energy appears to be weakly dependent on the laser wavelength. Laser tuning is not strictly continuous. As configured,

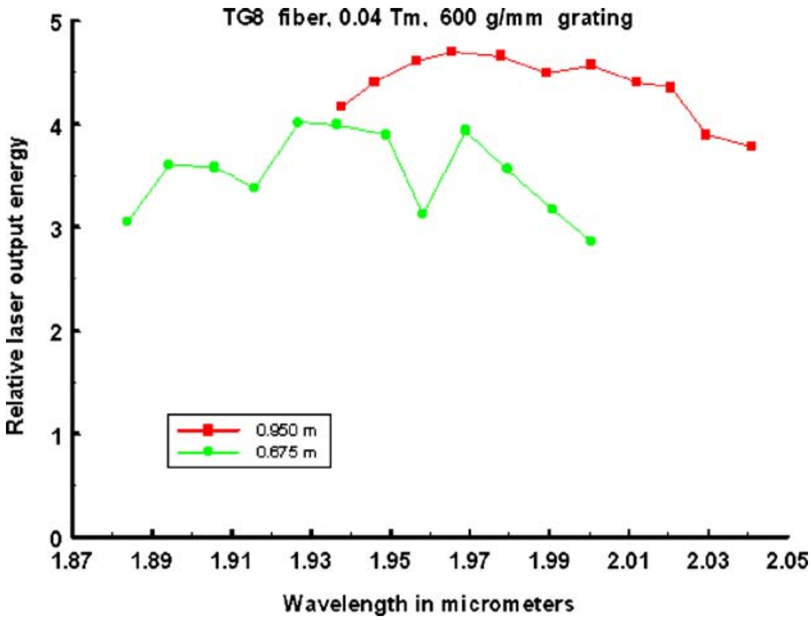

FIGURE 9 Tuning capability of Tm:germanate

Parameter	Threshold (mJ)	Slope efficiency
Correlation	0.9786	0.9937
Intercept	74.7	0.1898
Slope	0.608	−0.00397

TABLE 1 Laser performance vs. pulse repetition frequency

the laser resonator contains a lot of air in it. Consequently, the laser will not operate at wavelengths corresponding to strong atmospheric absorption features. This confirms the fact that the Tm:germanate fiber laser can indeed tune to atmospheric absorption features. For example, strong absorption features around 1.9 μm are clearly accessible.

The threshold increases and the slope efficiency decreases as the pulse repetition frequency increases. Most of the data presented above is taken at a pulse repetition frequency of 2.0 Hz. Here normal mode performance was evaluated as a function of the pulse repetition frequency between 1.0 and 10.0 Hz. Laser performance was fit to a linear relation to determine threshold and slope efficiency as a linear function of pulse repetition frequency. Results are given in the Table 1.

No effort was made to improve the heat sinking for this laser. The Tm:germanate fiber merely rested in a groove in a stainless steel plate.

5 Summary

Tm:germanate has proven to be an efficient and versatile fiber laser. When operated normal mode with a 5.0 ms pump pulse length, the laser was capable of producing a threshold less than 60 mJ and a slope efficiency approaching 0.3. Both normal mode and Q-switch operation were evaluated as a function of the pump pulse length. Thresholds for both modes of operation were quite similar. Conversely, slope efficiency for normal mode operation increases as the pump pulse length increases. However the slope efficiency for Q-switched operation decreases as the pump pulse length increases. Behavior for Q-switched operation can be described if there is nonlinear decay of the upper laser level. Nonlinear behavior can be caused by up conversion or amplified spontaneous emission.

Tm:germanate can operate at wavelengths between 1.88 and 2.04 μm. The tuning range depends on the length of the fiber. Multiple Q-switched pulses can be obtained from a single pump pulse. Multiple pulses, closely spaced in time, are needed for DIAL applications.

REFERENCES

1 N.P. Barnes, B.M. Walsh, S. Jiang, Spectroscopy of Tm:germanate for fiber lasers, Coherent Laser Radar Conference, Kamakura, Japan (2005)
2 B.M. Walsh, N.P. Barnes, D.J. Reichle, S. Jiang, J. Non-Cryst. Solids **352**, 5344 (2006)
3 R. Reisfeld, Y. Eckstein, J. Non-Cryst. Solids **12**, 357 (1973)
4 D. Di Martino, L.F. Santos, A.C. Marques, R.M. Almeida, J. Non-Cryst. Solids **394**, 293 (2001)
5 X. Zou, H. Toratani, J. Non-Cryst. Solids **195**, 113 (1996)
6 J.R. Lincoln, C.J. Mackechnie, J. Wang, W.S. Brocklesby, R.S. Deol, A. Pearson, D.C. Hanna, D.N. Payne, Electron. Lett. **28**, 1021 (1992)
7 J. Wu, S. Jiang, T. Luo, J. Geng. N. Peyghambarian, N.P. Barnes, IEEE Photon. Technol. Lett. **18**, 334 (2006)
8 N.P. Barnes, B.M. Walsh, D.J. Reichle, Assymetric time constants, CLEO Conference, Baltimore, MD (2007)